Chapter 5

Stability study of the proposed controller

5.1 Introduction

In the last chapter details of the hardware setup based on the proposed roof-top wind energy conversion system has been discussed. Also, the implementation of the generator field-weakening based DC-link voltage controller has been discussed. It is a typical process of conducting the stability study of any controller to comment upon the stability of the complete system. The following section conducts the stability study of the proposed controller.

5.2 Transfer function model of proposed RWECS

Fig. 5.1 shows the control circuit diagram of the proposed DCV controller based on proposed model as given in Fig. 4.1. However, to simplify the control circuitry, a resistive load has been used to load the generator in place of an induction motor load. The mathematical models of the physical systems are as follows. Eq. 5.1 presents the

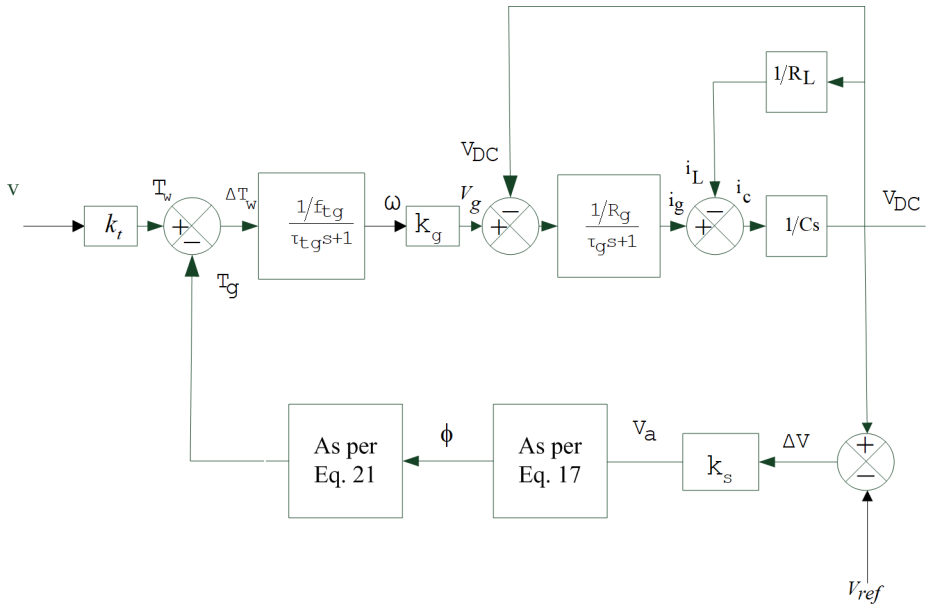

Fig. 5.1 Control circuit diagram of the proposed DC-link voltage controller.

mechanical dynamics of turbine-generator coupling.

$$T_t(t) - T_g(t) = J_{tg}\frac{d\omega(t)}{dt} + f_{tg}\omega(t) \tag{5.1}$$

T_t is the WTE torque, T_g is the generator electromagnetic torque, J_{tg} is the combined inertia of turbine-generator mechanical coupling while f_{tg} is the combined viscous friction force of turbine-generator against its rotor speed, and ω is the rotor speed in rad/sec. Taking the Laplace transform of the above equation

$$\frac{\omega(s)}{\Delta T(s)} = \frac{1}{J_{tg}s + f_{tg}} = \frac{1/f_{tg}}{\tau_{tg}s + 1} \tag{5.2}$$

Here, τ_{tg} is the time constant of the turbine-generator model. Furthermore, the generator output voltage, V_g, is directly proportional to the rotor speed and is given by Eq. 5.3 and 5.4

$$V_g(t) = k_g \omega(t) \tag{5.3}$$

$$V_g(s) = k_g \omega(s) \tag{5.4}$$

Here, k_g is the voltage constant of the generator that depends upon the air-gap flux linkage with the armature winding.

The wind generator three-phase output is then rectified through a three-phase rectifier and filtered by a DC-bus bar capacitor, C. The load, R_L, is then directly fed by a DC transmission line or inverted to AC power and then distributed through an AC distribution line. Eq. 5.5 represents the electrical transients.

$$V_g(t) - V_{DC}(t) = L_g \frac{di_g(t)}{dt} + i_g(t) R_g \tag{5.5}$$

Here, L_g and R_g are generator armature leakage inductance and resistance, respectively. Furthermore, the generator output current, i_g is divided among capacitive current i_c and load current i_L as in Eq. 5.6. Eq. 5.7 and 5.8 give the expression of capacitive current and load current.

$$i_g(t) = i_L(t) + i_C(t) \tag{5.6}$$

$$i_C(t) = C \frac{dV_{DC}(t)}{dt} \tag{5.7}$$

$$i_L(t) = \frac{V_{DC}(t)}{R_L} \tag{5.8}$$

Furthermore, taking the Laplace transform of Eq. 5.5-5.8, the transfer function is written as in Eq. 5.9.

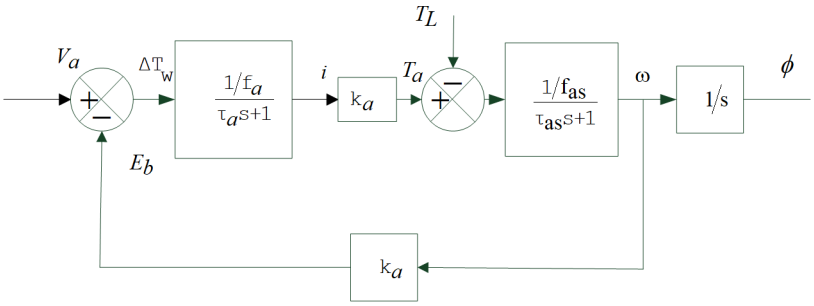

Fig. 5.2 Simplified mathematical model of stepper motor.

$$\frac{V_{DC}(s)}{V_g(s)} = \frac{R_L}{(L_g s + R_g)(CR_L s + 1) + R_L} \tag{5.9}$$

The DC-link voltage is then compared to a reference voltage, V_{ref}, and generates a control signal for the mechanical actuator.

The actual mechanical actuator used in the experimental setup is a two winding stepper motor. Fig. 5.2 presents a simplified mathematically model of the stepper motor [140, 141], and Eq. 5.10 gives the transfer function of the model.

$$\frac{\phi(s)}{V_a(s)} = \frac{k_a/R_a f_{as}}{s((\tau_a s + 1)(\tau_{as} s + 1) + k_a^2/R_a f_{as})} \tag{5.10}$$

Here, ϕ is Stator displacement angle (SDA) and Va, is the external supply to the stepper motor, τ_a is the electrical time constant of the stepper motor, and L_a and R_a are the leakage inductance and resistance of the armature winding. k_a is the voltage constant of the actuator. The mechanical actuator rotates the generator RS, and therefore, the actuator and the RS are coupled to each other. Thus, τ_{as} represent the combined time constant of the actuator-RS system, and f_{as} is the combined viscous friction force coefficient against the rotation.

The mechanical actuator is excited through a driver upon receiving the DC-link voltage error signal. The driver, thus, feeds the stepper motor through an external supply V_a. The approximate mathematical model of the driver has no time delay. Thus, represented by Eq. 5.11

$$\delta V_{DC}(s)k_s = V_a(s) \tag{5.11}$$

Also, Eq. 5.12 gives the active power of the wind generator.

$$P_g(t) = V_g(t)I_L(t) = \frac{V_g^2(t)}{R_L} \tag{5.12}$$

Where, as per Eq. 3.2

$$V_g(t) = V_o \cos(\frac{\phi}{2})) \tag{5.13}$$

Therefore, the generator power reduces by a factor $\cos^2(\phi/2)$. Thus, the generator torque equation is given as Eq. 5.13

$$T_g(t) = \frac{P_g(t)}{\omega(t)} \tag{5.14}$$

$$T_g(t) = \frac{k_g^2 \omega \cos^2(\phi/2)}{R_L} \tag{5.15}$$

The generator torque is a nonlinear function. Thus, the torque equation is linearized around an operating point $\omega = \omega_o$ and $\phi = 90^o$ by Taylor's equation. Eq. 5.16 gives the final expression.

$$\delta T_g(t) = k_g^2 \omega_o(-\phi(t)) \tag{5.16}$$

As per Eq. 5.16, upon rotation of the rotatable stator by ϕ electrical angle the change in torque is negative. Here, it should be noted that the generator torque feedback is negative feedback, invariant to the operating region of the wind turbine.

Fig. 5.3 presents a simplified control circuit diagram involving all the equations. It is to be noted that in the control circuit diagram, the summer between the turbine and generator has been shifted to the left to simplify the whole system into its open-loop gain G(s) and feedback H(s) as per Fig. 5.4.

Eq. 5.17 and 5.18 give expressions of G(s) and H(s), respectively.

$$G(s) = \frac{(k_g R_L K_t)/(f_{tg} R_g)}{(\tau_{tg} s + 1)((\tau_g s + 1)(C R_L s + 1) + R_L/R_g)} \tag{5.17}$$

$$H(s) = \frac{(K_s K_a K_g^2 \omega_0)/(K_t R_a f_{as})}{s((\tau_a s + 1)(\tau_{as} + 1) + K_a^2/(R_a f_{as}))} \tag{5.18}$$

$$T(s) = \frac{V_{DC}(s)}{V(s)} = \frac{G(s)}{1 + H(s)G(s)} \tag{5.19}$$

$$1 + G(s)H(s) = 0 \tag{5.20}$$

Eq. 5.19 represents the final transfer function, whose characteristic equation is given by Eq. 5.20. The characteristic equation is found to be of sixth-order. Therefore, to reduce the order of the function following assumption are taken into consideration

1. Generator electrical time constant is neglected in comparison to turbine-generator mechanical time constant [142].

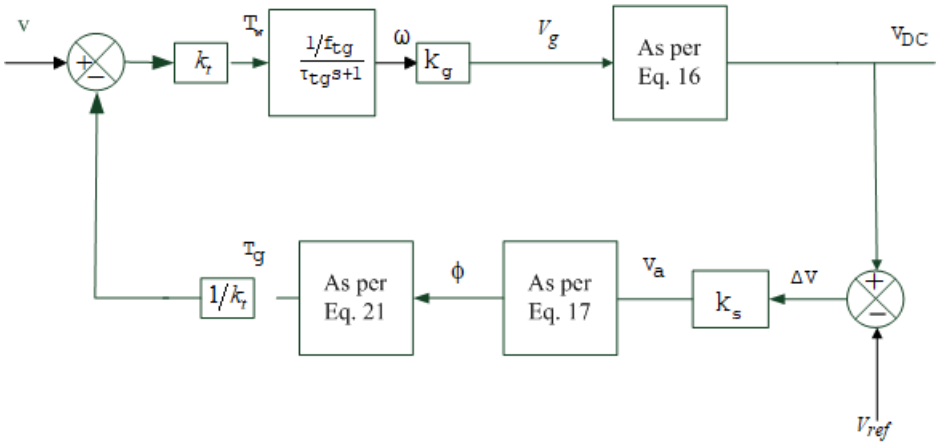

Fig. 5.3 Simplified control circuit diagram of the Proposed system.

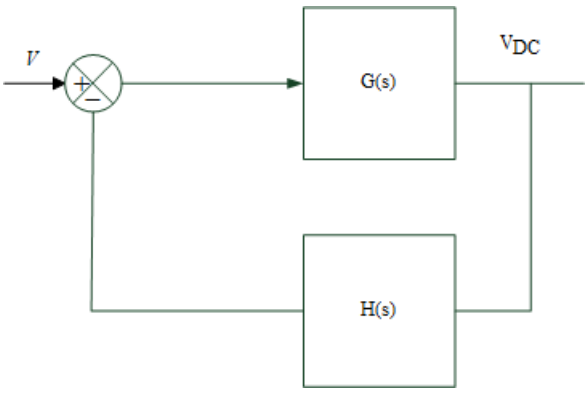

Fig. 5.4 Final control circuit diagram of proposed controller.

2. Similarly, actuator electrical time constant is neglected in comparison to actuator-RS mechanical time constant.

A reduced-order expression of G(s) and H(s) are as follows

$$G(s) = \frac{(k_g R_L K_t)/(f_{tg} R_g)}{(\tau_{tg} s + 1)(C R_L s + 1 + R_L/R_g)} \tag{5.21}$$

$$H(s) = \frac{(K_s K_a K_g^2 \omega_0)/(K_t R_a f_{as})}{s(\tau_{as} s + 1 + K_a^2/(R_a f_{as}))} \tag{5.22}$$

Thus, the characteristic equation reduces to a fourth-order equation. Rewriting the equation and represented as in Eq. 5.23 and 5.24

$$G(s) = \frac{K_{ng}}{(\tau_{tg} s + 1)(C R_L s + 1 + K_{dg})} \tag{5.23}$$

$$H(s) = \frac{K_{nh}}{s(\tau_{as} + 1 + K_{dh})} \tag{5.24}$$

$$T(s) = \frac{G(s)}{1 + H(s)} \tag{5.25}$$

Here, k_{dg} and k_{dh} are large quantities in comparison to mechanical time constant τ_{as} and τ_{tg} owing to low values of R_g and R_a.

5.3 Time-domain stability analysis

The stability of the transfer function modelled in by Eq. 5.25 can be studied in the time-domain or frequency-domain. In some work [143–145], the stability of the transfer function has been studied using frequency domain analysis. In [143–145], the controlled variable is studied at high frequency, such as closing and opening of a valve in an internal combustion engine. In such type of systems, frequency domain analysis is preferred [146].

However, in this paper, the system dynamics is slow owing to the high time constant of the wind velocity and the mechanical systems. Therefore, in this system, time-domain analysis has been preferred.

Here, the stability test of the proposed controller uses the Routh-Hurwitz stability criterion. The necessary equations are given in the appendix. For the controller to be stable, quantities such as a_0, a_1, b_1, c_1, and d_1 should be positive. Variable a_0, a_1, and d_1 are easily identified as to be positive. For b_1, the positive part of the expression a_1a_2 contains expressions with third degrees of high quantities, such as k_{dg} and k_{dh}. On the other hand, the negative part of b_1 contains the expression of two degrees of the same quantities k_{dg} and k_{dh}. Therefore, b_1 is bound to be positive in all real systems. For c_1 also, the same logic follows.

In the controller, the mechanical actuator rotates generator-RS in a direction to maintain V_{DC} at V_{ref} and, thus, apply negative feedback in the control logic at all conditions.Therefore, any system based on the proposed controller is stable invariant to the operating region of the wind turbine. The reason is due to the inherent property of the control logic of giving negative feedback at all operating conditions.

5.4 Conclusion

In this chapter the steady state stability study of mechanical field-weakening based DC-link voltage controller in the proposed roof-top wind energy conversion system has been conducted. The proposed system has been found stable invariant to the operating region of the wind turbine. In the next chapter experimentations have been performed on the hardware setup to validate the principle of concept of this thesis.